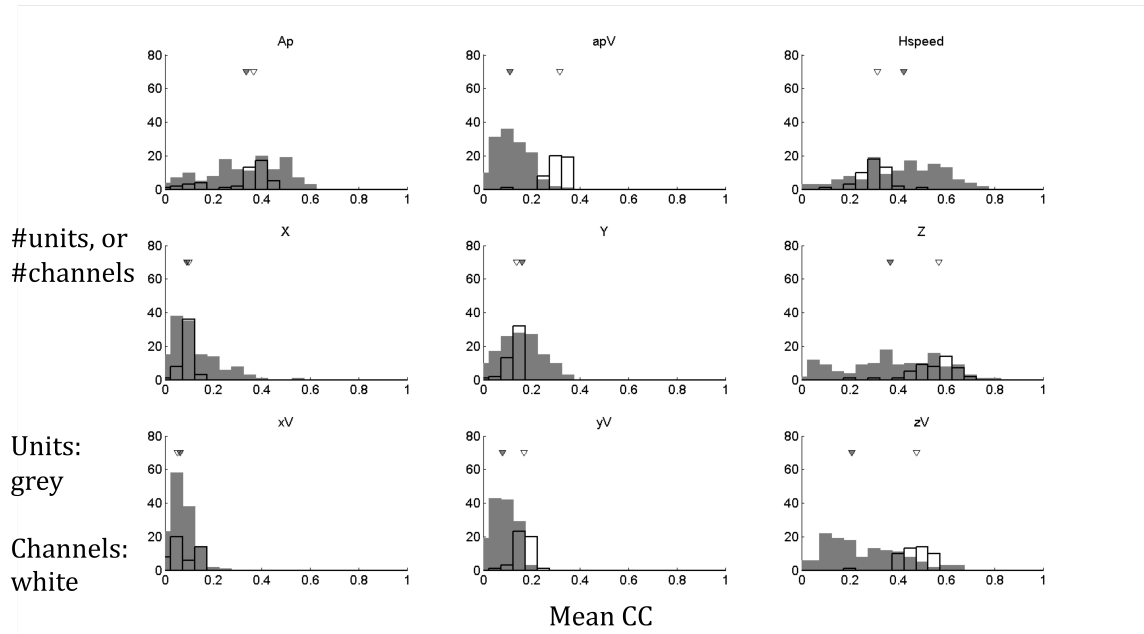
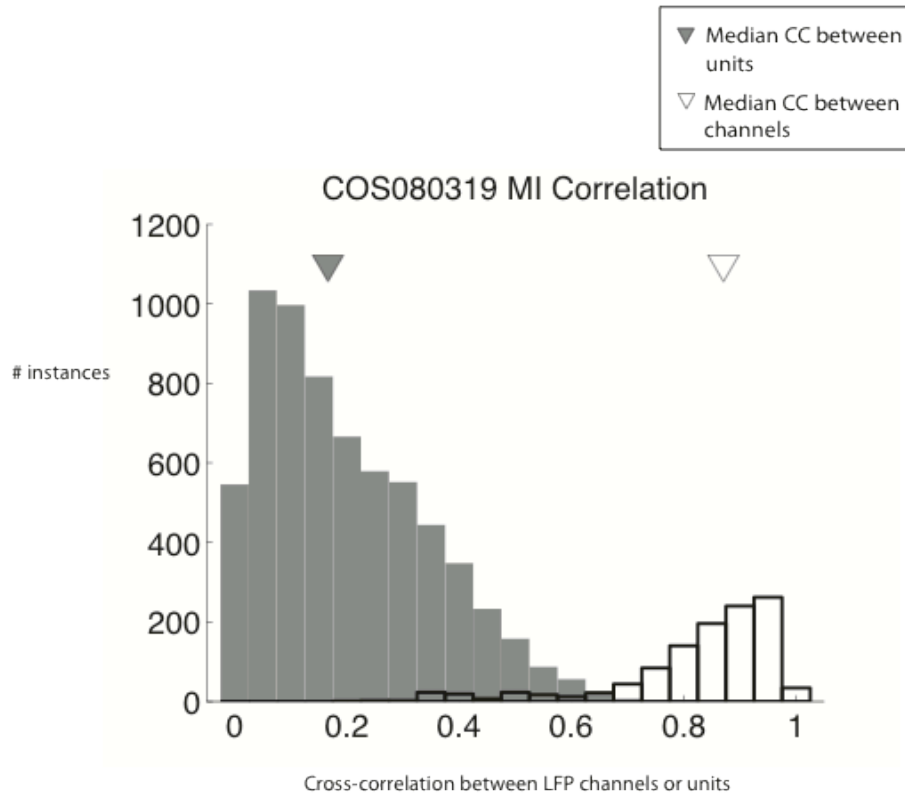


Supplementary Figure 2a: Comparison of individual units vs individual channel decoding performance. Distribution of cross-correlations when using individual units (grey) versus using individual lf-LFP channels (white). Inverted triangles represent the corresponding medians of the distributions. For all comparisons (except x-position and x-velocity, where $p > 0.75$), the medians were significantly different ($p < 10^{-11}$, Kruskal-Wallis test). (**Monkey G, Session 2, PMv array**).

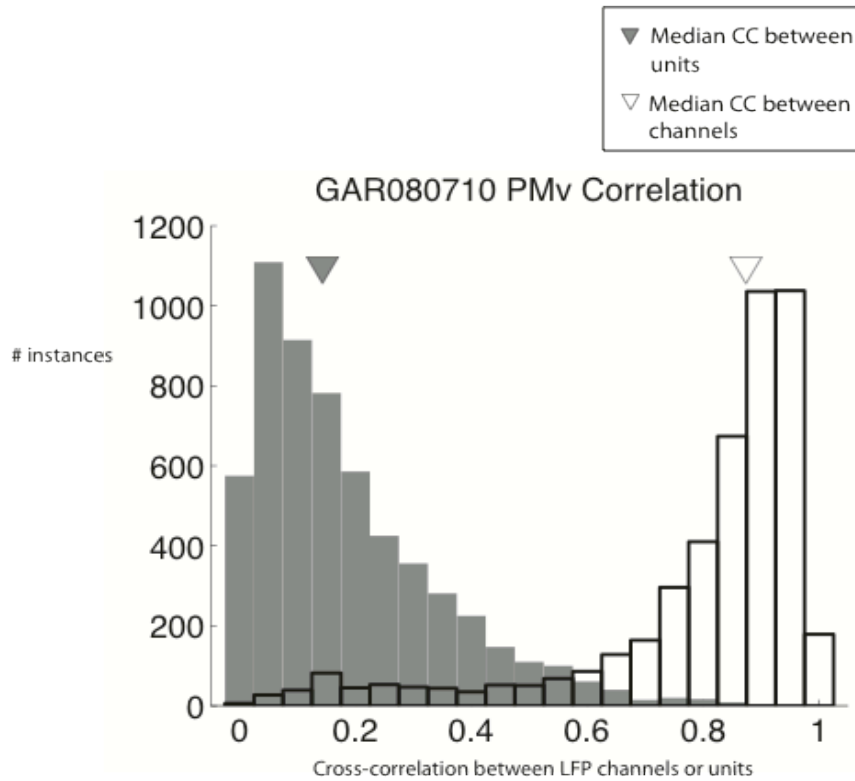


Supplementary Figure 2b: Comparison of individual units vs individual channel decoding performance. Distribution of cross-correlations when using individual units (grey) versus using individual lf-LFP channels (white). Inverted triangles represent the corresponding medians of the distributions. For all comparisons (except aperture, x-position and x-velocity, where $p > 0.5$), the medians were significantly different ($p < 10^{-4}$, Kruskal-Wallis test, except y-position where $p < 0.05$). (Monkey C, Session 1, MI array).

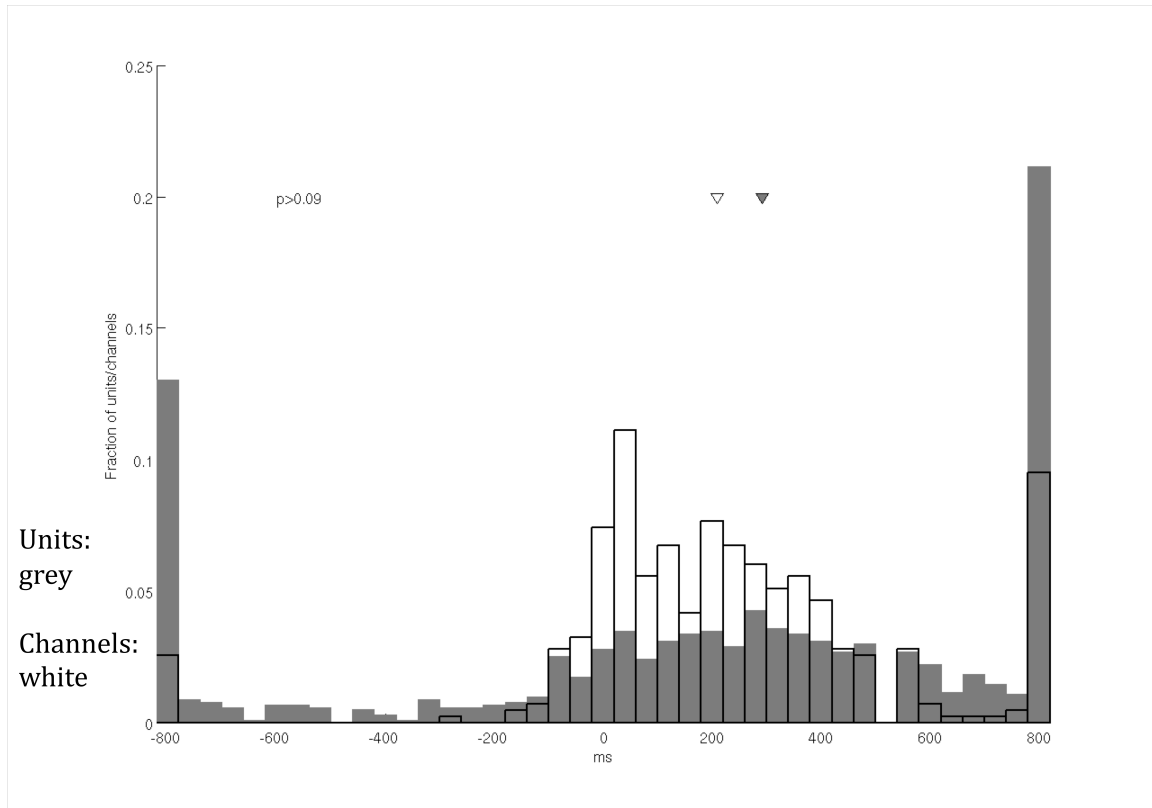
Supplementary Figure 3 a)



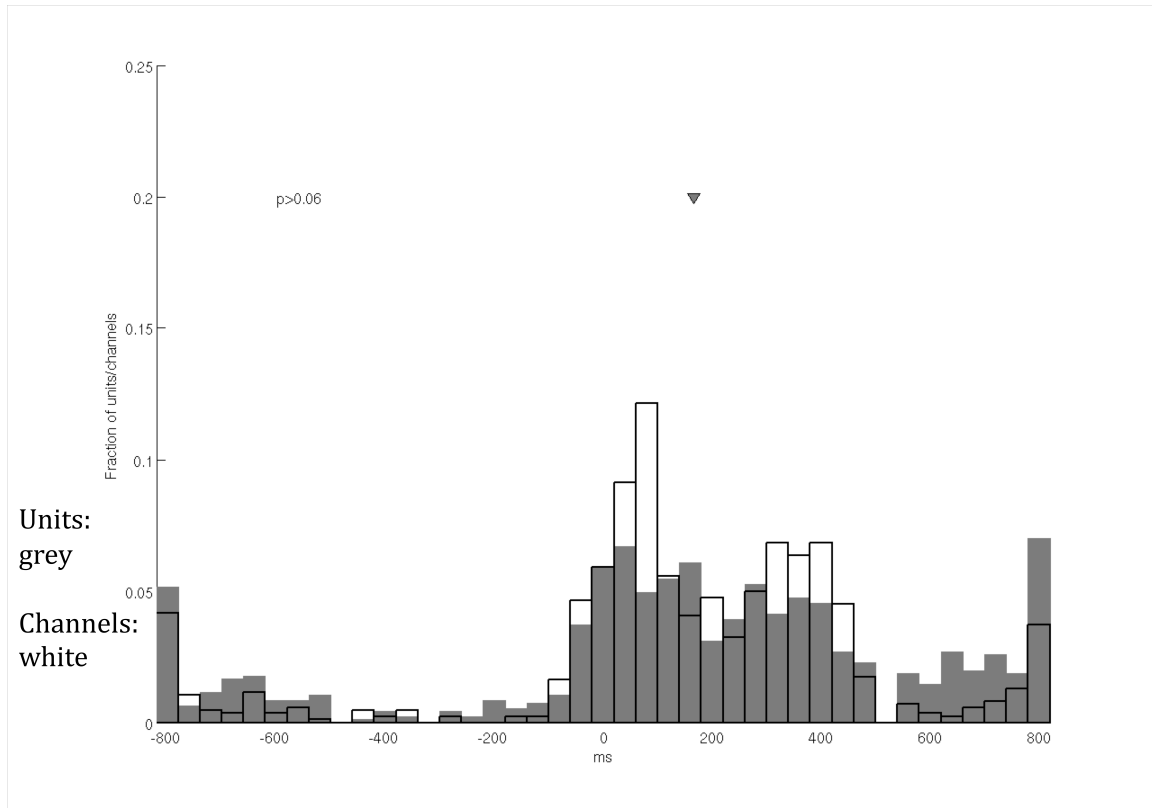
b)



Supplementary Figure 3: Relative independence of *lf*-LFPs and spiking units. Histograms of correlation-coefficient (Pearson's r) between all pairs of simultaneously recorded *lf*-LFPs (white), or all pairs of simultaneously recorded spiking units (grey) during (a) Monkey C, MI, Session 2, and (b) Monkey G, PMv, Session 2.



Supplementary Figure 4a: Comparison of individual unit versus individual channel optimal lags (Monkey C, Session 2, MI). Distribution of channels/units with different optimal lags. Inverted triangles represent median optimal lag. Grey: Units; White: Channels.



Supplementary Figure 4b: Comparison of individual unit versus individual channel optimal lags (Monkey G, Session 2, PMv). Distribution of channels/units with different optimal lags. Inverted triangles represent median optimal lag. Grey: Units; White: Channels.